

The first direct experimental comparison between the hugely contrasting properties of PEDOT and the all-sulfur analogue PEDTT by analogy with well-defined EDTT–EDOT copolymers†

Howard J. Spencer,^a Peter J. Skabara,^{‡,*a} Mark Giles,^b Iain McCulloch,^b Simon J. Coles^c and Michael B. Hursthouse^c

Received 3rd August 2005, Accepted 5th September 2005

First published as an Advance Article on the web 3rd October 2005

DOI: 10.1039/b511075k

The structures of poly(3,4-ethylenedioxythiophene) (PEDOT) and poly(3,4-ethylenedithiathiophene) (PEDTT) vary only in the substituent chalcogen atoms, yet the electronic properties of the materials are surprisingly dissimilar. The difference in electronic band gaps is approximately 0.8 eV and the polymers behave very differently upon p-doping. Two new terthiophenes have been synthesised using Negishi coupling methods. The X-ray crystal structures of EDOT–EDTT–EDOT (OSO) and EDTT–EDOT–EDTT (SOS) show strong intramolecular chalcogen–chalcogen contacts which are responsible for persistent conformers in solution and solid state, although significant interchain interactions should also influence the properties of the materials. SOS and OSO can be polymerised by electrochemical oxidation to give the corresponding, well-defined poly(terthiophenes) PSOS and POSO. Spectroelectrochemical studies on all four polymers reveal strong similarities between PEDTT and PSOS, and between PEDOT and POSO. Together with independent electrochemical and absorption studies, the results indicate that the unique properties of PEDOT are influenced more by conformational effects (intrachain S⋯O contacts) than substituent effects.

Introduction

Poly(ethylene-3,4-dioxythiophene) (PEDOT) has become one of the most popular polythiophene derivatives used for device applications, due to its exceptional hole injection properties, high conductivity and stability.¹ The ionic nature and high solubility of the doped analogue PEDOT-poly(styrenesulfonate) (PEDOT PSS) enable one to process the material from water and are therefore desirable for multilayer device processing. Since the polymer was first reported in the late 1980s/early 1990s,^{2,3} numerous variants of EDOT and PEDOT have been investigated. Bayer AG began the multi-ton production of EDOT under the trade name Baytron[®] M in 1998 which was passed to H. C. Stark in 2003. Applications of PEDOT include antistatic coatings for CRTs, photographic film, and electronics packaging. PEDOT has also emerged as an effective hole injecting layer when deposited on electrodes within OLEDs.^{4,5} Polymers of EDOT offer high thermal stability, conductivity in the order of several hundred S cm^{−1} and form highly stable⁶ pale blue transparent films when

doped. In the undoped state, the polymer is a dark blue material; PEDOT and its derivatives are therefore highly suitable for electrochromic applications such as smart windows and displays.⁷

Much of the research associated with EDOT has entailed the incorporation of the EDOT core into copolymers, or by varying the bridging alkyl groups to give alternative alkoxy structures.^{8–21} In contrast to the vast amount of research that has followed the original findings of the Bayer laboratories, there is an apparent lack of research devoted to the sulfur analogue of EDOT, 3,4-ethylenedithiathiophene (EDTT). Kanitzidis *et al.*²² first described the synthesis of EDTT from thieno[3,4-*d*]-1,3-dithiole-2-thione and detailed the chemical and electrochemical polymerisation of the monomer, together with the characterisation of the polymer in the doped and dedoped states. An alternative preparation to various 3,4-bis(alkylthio)thiophenes, including EDTT, is given by Meijer *et al.*²³ In relation to this work, we have reported the synthesis and electropolymerisation of the terthiophenes 2,5-di(2-thienyl)-3,4-(ethylenedisulfanyl)thiophene **1** and 2,5-di(2-thienyl)-3,4-(propylenedisulfanyl)thiophene **2**²⁴ and described the spontaneous solid state polymerisation of 2,5-dibromo-3,4-ethylenedithiathiophene **3** which yields PEDTT in its doped state.²⁵ Remarkably, there is a large difference between the optical and redox properties of PEDOT and PEDTT, which is due to the influence of the chalcogen atoms at the 3- and 4-positions of the thiophene ring.

In this work, we investigate the effect of successive replacement of oxygen atoms for sulfur in the basic PEDOT structure. This has been made possible by the synthesis of two new

^aDepartment of Chemistry, University of Manchester, Oxford Road, Manchester, UK M13 9PL. E-mail: peter.skabara@strath.ac.uk

^bMerck Chemicals, Chilworth Science Park, Southampton, UK SO16 7QD

^cDepartment of Chemistry, University of Southampton, Highfield, Southampton, UK SO17 1BJ

† Electronic supplementary information (ESI) available: synthesis of EDOT. See DOI: 10.1039/b511075k

‡ New address: Department of Pure and Applied Chemistry, University of Strathclyde, 295 Cathedral Street, Glasgow, UK G1 1XL.

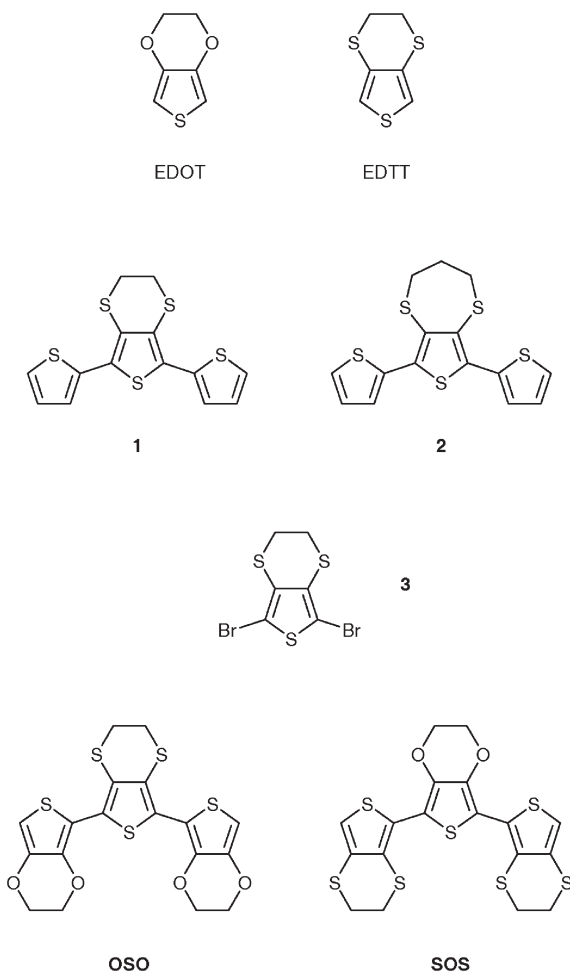


Chart 1

terthiophenes, **OSO** and **SOS**, which possess a core EDOT or EDTT unit and two outer, opposing units. Electropolymerisation of these compounds, along with that of EDOT and EDTT, has enabled us to study the electronic properties of polymers with varying composition of EDOT/EDTT units, passing from pure PEDOT to pure PEDTT *via* 1 : 2 and 2 : 1 mixed systems.

Synthesis

The synthesis of EDOT was achieved using the Mitsunobu coupling route (Scheme 1) and an account of this procedure is given in the Electronic Supplementary Information (ESI†). Bromination of EDOT was effected by the addition of NBS to the starting material in a solution of DCM and acetic acid at 0 °C (51%). Finally, the terthiophenes were formed by addition of 2,5-dibromo(EDOT)¹⁹ (**4**) or 2,5-dibromo(EDTT)²⁵ (**3**) to a THF solution of mono-lithiated EDTT or EDOT and were coupled *via* the Negishi approach (ZnCl₂–Pd(PPh₃)₄) in 9% (**OSO**) and 7% (**SOS**) yields.

X-Ray crystallography

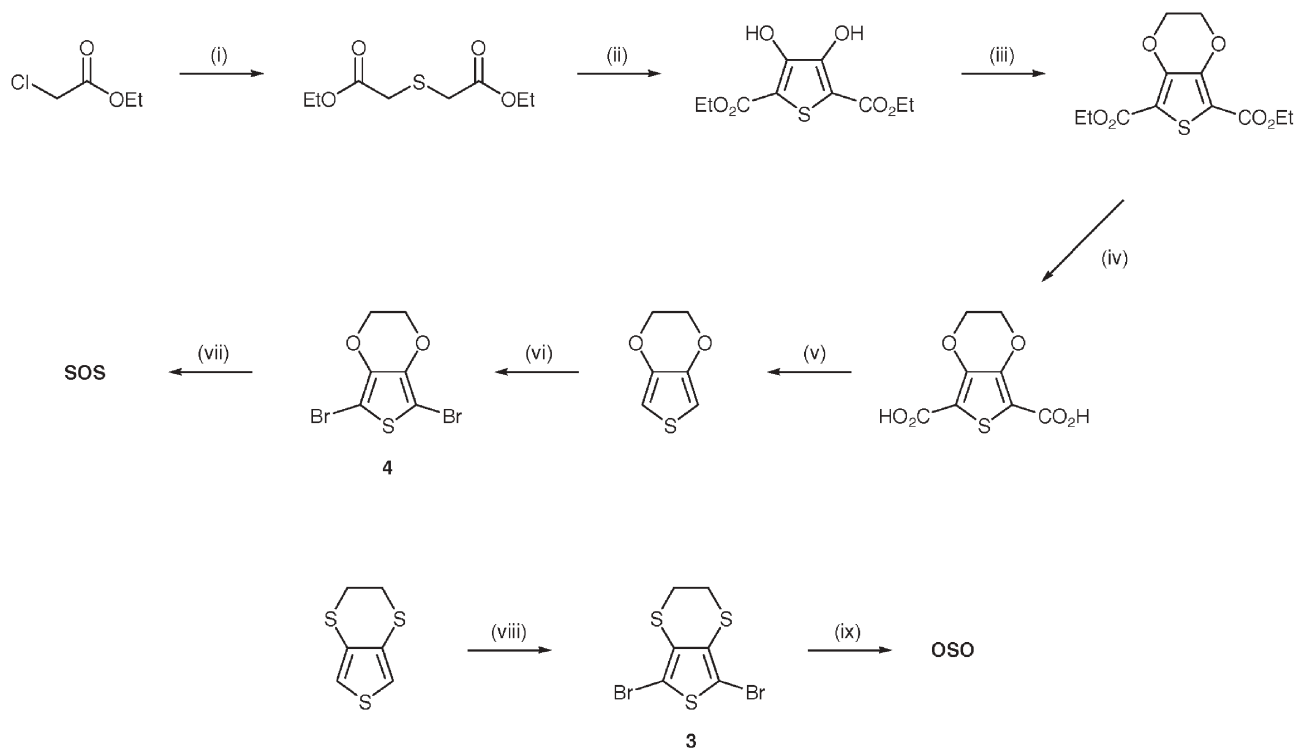
The two new terthiophenes, **OSO** and **SOS**, both adopt the all-*anti* conformation (Fig. 1), which is aided by the existence

of S⋯O and S⋯S short intramolecular contacts between the thiophene sulfurs and the sulfur or oxygen at the 3,4-positions of each thiophene. In compound **OSO** (Fig. 1a), the distance between S(1)⋯O(1) is 2.930(4) Å and that between S(1)⋯O(3) is 3.175(11) Å. These contacts are significantly shorter than the sum of the van der Waals radii for oxygen and sulfur (3.32 Å²⁶) and are partly responsible for the conformation of the molecule in the solid state. However, the molecule is twisted out of coplanarity between adjacent rings, with maximum torsion angles of 30.81(13)° (S(4)–C(7)–C(4)–S(1)) and 45.08(15)° (S(5)–C(13)–C(1)–S(1)). The sulfurs of the central dithioethylene bridge interact with those of the adjacent EDOT units, giving close contacts between S(3)⋯S(4) (3.185(1) Å) and S(2)⋯S(5) (3.310(4) Å). There are no significant intermolecular contacts observed in the structure of **OSO**.

Compound **SOS** shows a good degree of planarity between the central EDOT and the right-hand EDTT ring (3.82(33)°; S(3)–C(6)–C(7)–S(4), Fig. 1b). The corresponding S⋯O (2.793(4) Å) and S⋯S interactions (3.096(2) Å) for the coplanar pair are significantly shorter than those at the other side of the molecule (S(5)⋯O(2), 3.194(4) Å; S(4)⋯S(7), 3.345(2) Å), where a prominent twist exists (48.96(41)°; S(5)–C(13)–C(10)–S(4)). The drive towards rigidification in the terthiophenes is not hindered by a high rotational energy barrier, which is usually of the order of 10–20 kJ mol^{–1},²⁷ so it is feasible that the preferred conformation is due to packing forces in the crystal lattice. As in the case of **OSO**, there are no significant intermolecular interactions for compound **SOS**.

Electronic absorption spectra (monomers)

The electronic absorption spectra in dichloromethane for the monomeric species are shown in Fig. 2. The absorption maxima for EDOT (258 nm) and EDTT (289 nm) reveal a distinct red shift for the latter (31 nm), as expected for an *S*-alkyl derivative. A much larger bathochromic shift is observed when we examine the terthiophenes **OSO** and **SOS** and this is due to the elongation of the conjugated unit in each case. Both spectra exhibit detailed structure within the π–π* band, indicative of ordering in the solution state and presumably arising from the intramolecular chalcogen–chalcogen interactions observed in the crystal structures. The relative peaks are 367, 386 and 409 nm for **OSO** and 380, 399 and 425 nm for **SOS** and the differences between the two compounds are as expected for an increased number of sulfur atoms. Similar fine structure has been observed in the absorption spectra of tetra- and difluorophenylene-thiophene derivatives in which there are strong intramolecular S⋯F and H⋯F interactions, resulting in highly planar molecules.²⁸ In support of the assumption that the EDOT unit is key to the rigidification process, thiophene–EDTT–thiophene **1**²⁴ (which is analogous to compound **OSO**) displays an absorption maximum at 368 nm (in dichloromethane), with no additional features. Indeed, the crystal structure of **1** reveals an all-*syn* conformation for the terthiophene, with no intramolecular S⋯S interactions involving the ethylenedithio bridge.



Scheme 1 Reagents and conditions: (i) $\text{Na}_2\text{S}\cdot 9\text{H}_2\text{O}$, acetone, $60\text{ }^\circ\text{C}$, 3 h; (ii) NaOEt , 0.5 h, $(\text{CO}_2\text{Et})_2$, reflux, 18 h, 2 M HCl ; (iii) PPh_3 , ethylene glycol, DEAD, reflux, 18 h; (iv) KOH , EtOH , reflux, 3 h; (v) Cu(II)O , quinoline, $200\text{ }^\circ\text{C}$, 5 h; (vi) NBS , $\text{DCM} : \text{AcOH}$ (3 : 1), $0\text{ }^\circ\text{C}$, 3 h, in the dark; (vii) EDTT, $n\text{-BuLi}$, ZnCl_2 , $\text{Pd(PPh}_3)_4$; (viii) NBS , $\text{DCM} : \text{AcOH}$ (3 : 1), $0\text{ }^\circ\text{C}$, 3 h, in the dark; (ix) EDOT, $n\text{-BuLi}$, ZnCl_2 , $\text{Pd(PPh}_3)_4$.

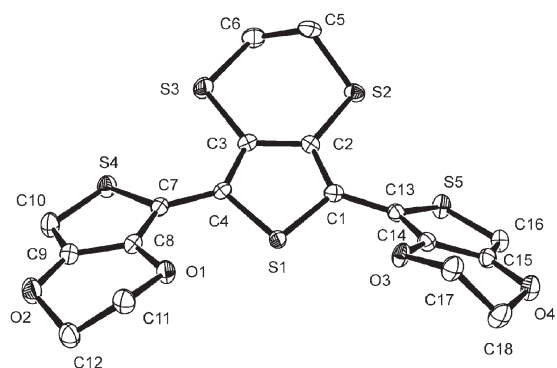
Electrochemistry

EDOT, EDTT and the two terthiophenes, **OSO** and **SOS**, have been studied by cyclic voltammetry in dichloromethane solution using a Ag/AgCl reference electrode and tetrabutylammonium hexafluorophosphate as the supporting electrolyte. Under these conditions, the single thiophene derivatives display one-electron irreversible oxidation peaks at +1.55 V (EDOT) and +1.57 V (EDTT). The cyclic voltammograms of the terthiophenes are shown in Fig. 3. Compound **SOS** undergoes an irreversible oxidation process at +0.70 V and the sharp reduction peak at +0.12 V represents good stability of the cation radical, possibly due to a stabilising conformational change upon oxidation.²⁹ In contrast, **OSO** affords a small peak at +0.1 V, a broad oxidation peak at +0.37 V and a sharper, third oxidation peak at +0.75 V. The complex electroactivity of **OSO** could be due to the presence of persistent conformers in solution, giving rise to stabilised radical cation species.

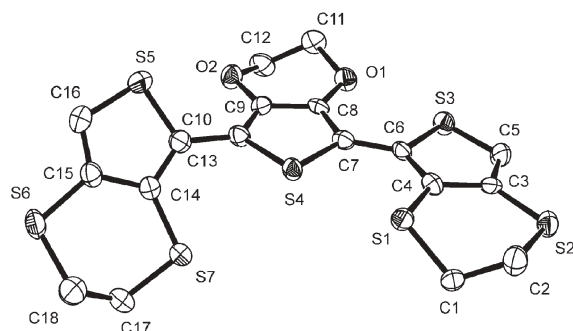
Both terthiophenes were electropolymerised, using the same solvent and conditions used for the cyclic voltammetry experiments, by repetitive cycling over the redox active range of the materials. PEDOT and PEDTT were also freshly prepared under the same conditions to allow an accurate comparison of the polymers' properties. In each case, the as-made polymers were dedoped for a period of one hour in a region of electrochemical inactivity in a monomer-free acetonitrile solution, containing the same concentration of electrolyte. The voltammetric range for this procedure was determined by a 50–100 mV drop with respect to the new

oxidation process displayed in the electrochemical polymerisation trace. The electropolymerisation of PEDOT⁹ and PEDTT²² has been reported previously. The growth traces for the terthiophenes **OSO** and **SOS** are displayed in Fig. 4. Whereas terthiophene **OSO** polymerised readily, **SOS** required 240 cycles of continual scanning between -0.6 and $+1.0$ V before a satisfactory film was obtained. It should be noted that the electropolymerisation of terthiophenes at relatively low oxidation potentials can lead to oligomeric (e.g. sexithiophene) products rather than long chain polymers and this could be the reason for the slow growth rate for **SOS**.³⁰ For each of the polymers, a plot of scan rate vs. current gives a linear fit (Fig. 5, $R = 0.996\text{--}0.999$), confirming that charge transport through the film is not diffusion limited.³¹

The electrochemistry of the four polymers was investigated in acetonitrile vs. Ag/AgCl . The cyclic voltammograms of PEDOT and PEDTT are shown in Fig. 6 and clearly show the remarkable difference in redox properties between the two polymers (see also Table 1). The electrochemical band gaps of the materials can be deduced from the difference between the onsets of reduction and oxidation processes. In the case of PEDTT, the band gap estimate agrees closely with the literature value (2.14–2.19 eV).²² Our electrochemical estimate of the band gap for PEDOT (1.35 eV, Fig. 6 and Table 1) is within the reported range (1.2–1.7 eV)^{2,32–35} whilst the optical determination of E_g coincides with that reported by Heinze *et al.* (1.6 eV).⁹ The differences in the band gaps for PEDTT and PEDOT are large, considering the common basic structure of the two polymers. This disparity is owed more to the conformation of the polymers than the inductive and



(a)



(b)

Fig. 1 X-Ray crystal structures of (a) compound **OSO** and (b) compound **SOS**, showing the asymmetric units with H atoms omitted for clarity.

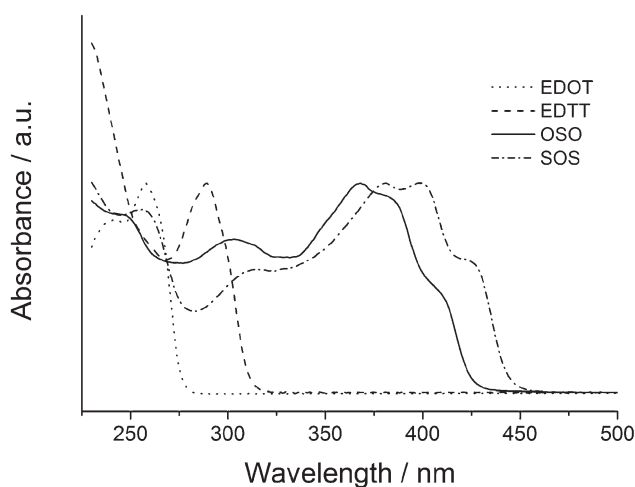


Fig. 2 Absorption spectra of monomers in dichloromethane solution.

resonance effects of the chalcogen substituents. Pure substituent effects are observed in the CVs of EDOT and EDTT, for which there is a difference of only 20 mV between oxidation potentials. However, the difference in E_{lox} between PEDOT and PEDTT is much larger at 780 mV. For PEDOT, chalcogen...chalcogen interactions (as seen in Figs. 1 and 7)

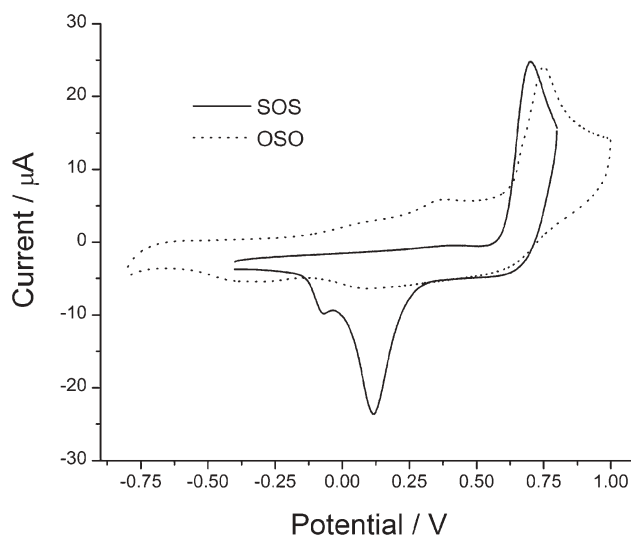
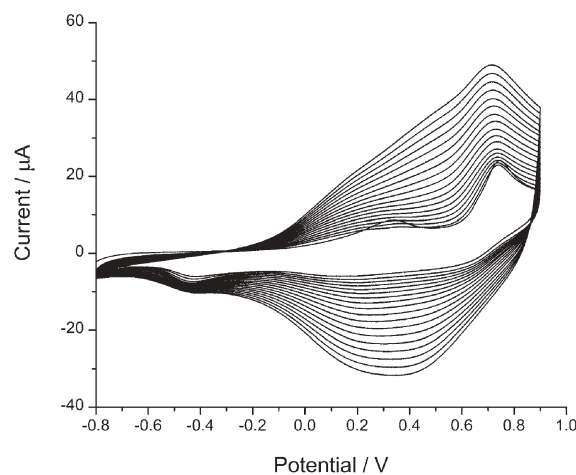
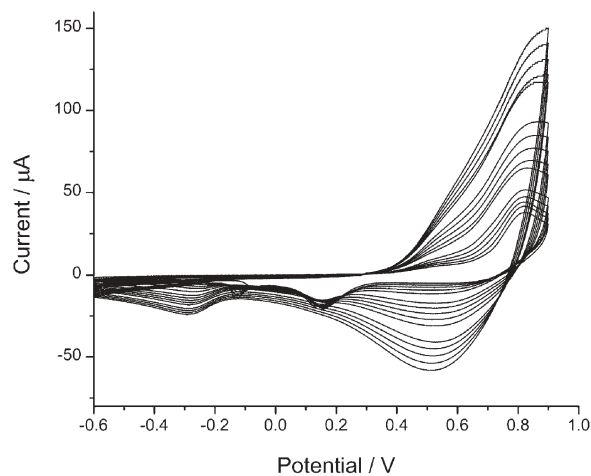


Fig. 3 Cyclic voltammograms of terthiophenes **SOS** and **OSO** in dichloromethane solution, using a glassy carbon working electrode, Ag/AgCl reference electrode, platinum counter electrode, substrate concentration 10^{-3} M, tetrabutylammonium hexafluorophosphate as supporting electrolyte (0.1 M) and a scan rate of 100 mV s^{-1} .



(a)



(b)

Fig. 4 Electrochemical growth of (a) **POSO** and (b) **PSOS**.

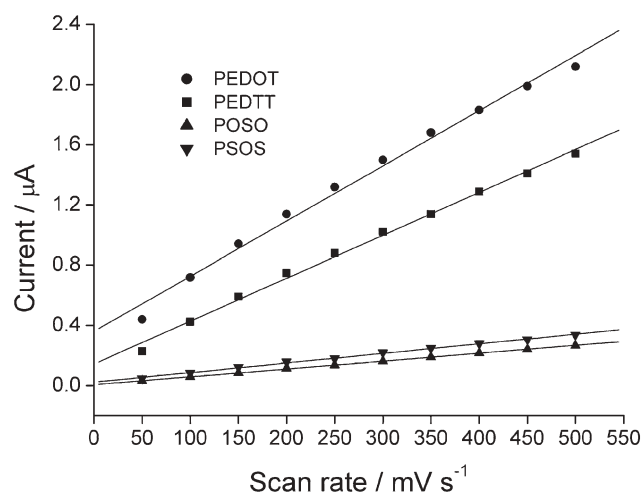


Fig. 5 Plot of current versus scan rate for polymers.

provide a certain degree of rigidification and therefore increased effective conjugation length. In the all sulfur analogue, PEDTT, adjacent units suffer from a competing steric interaction between the sulfur atoms. The electronic absorption spectra for the two polymers reflect this conformational effect. In the solid state, the absorption maximum of PEDOT is red-shifted by 137 nm with respect to that of PEDTT (Table 1). This is the reverse of the comparison between EDOT ($\lambda_{\text{max}} = 258$ nm) and EDTT ($\lambda_{\text{max}} = 289$ nm) for which there is a difference of 31 nm. For terthiophenes SOS and OSO, the conformational effect is already influencing the absorption characteristics. The positions of analogous peaks for OSO and SOS follow the same trend as for EDOT and EDTT, but the differences in values are reduced to 10–16 nm.

A comparison with the data for POSO and PSOS (Fig. 6 and Table 1) gives a closer insight into the role of substituents and the conformational effect. If we take into consideration an all-*anti* conformation for PEDOT (which has been found to be the global minimum at different levels of theory),³⁶ the structure will give exclusively O...S interactions between repeat units (Fig. 7). In the case of POSO, less favourable and sterically demanding S...S interactions are introduced, but the frequency of strong O...S contacts still allows for rigidification throughout the chain. Hence, the hypsochromic shift for the longest wavelength absorption maxima from PEDOT to POSO is fairly small (25 nm). A much larger shift is observed for PSOS (132 nm, *c.f.* PEDOT), but in this structure coplanarity through S...O contacts is restricted to

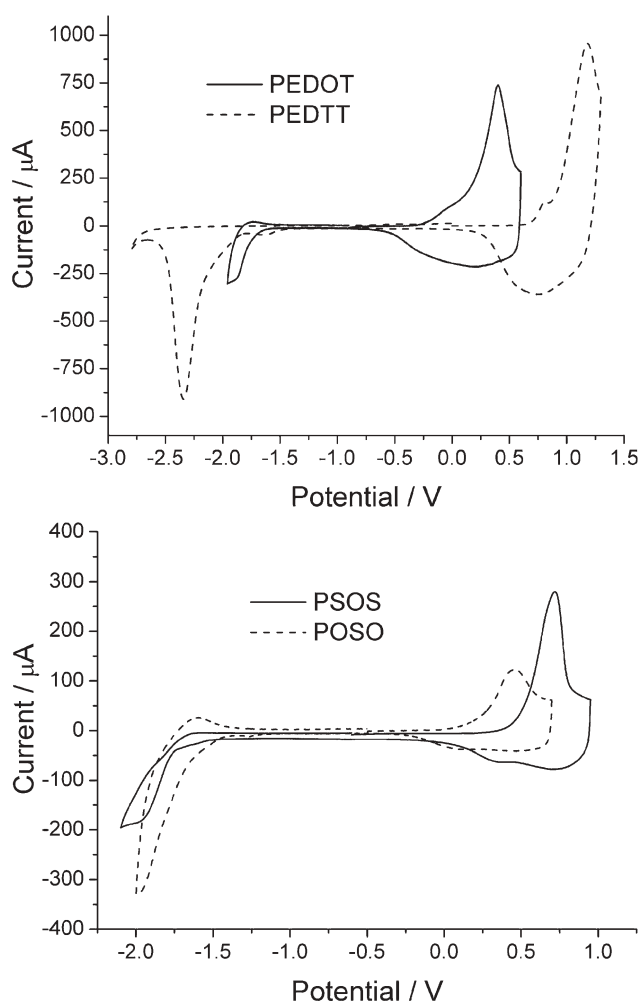


Fig. 6 Cyclic voltammograms of polymers as films on ITO glass. Experiments were conducted in monomer-free acetonitrile solution, under the same conditions as given in Fig. 3.

localised trimeric EDTT-EDOT-EDTT segments (Fig. 7). The trimer units do not provide a significant contribution to the overall mean conjugation length of the polymer, since there is only a small difference between the absorption maxima for PSOS and PEDTT (5 nm).

The electrochemical data for the four polymers do not follow the same degree of variance observed for the λ_{max} values and indicates a stronger contribution of substituent effects towards the HOMO/LUMO levels. The values for E_{1ox} tend toward a linear fit against the percentage composition of EDOT units in the polymer. However, planarity and

Table 1 Electrochemical and absorption data for polymers

Compound	E_{1ox}/V	E_{1red}/V	HOMO/eV ^a	LUMO/eV ^a	E_g/eV	$\lambda_{\text{max}}/\text{nm}$
PEDOT	+0.40	−1.89	−4.0	−2.7	1.35, ^b 1.63 ^c	578
PEDTT	+1.18	−2.34	−4.9	−2.75	2.19, ^b 2.15 ^c	441
POSO	+0.45	−1.94	−4.3	−2.8	1.47, ^b 1.64 ^c	553
PSOS	+0.72	−1.95	−4.6	−2.7	1.89, ^b 2.14 ^c	446

^a HOMO and LUMO values are calculated from the onset of the corresponding redox wave and referenced to ferrocene ($E^{1/2} = +0.54$ V), which has a HOMO of −4.8 eV. ^b Electrochemical band gap from the HOMO–LUMO separation. ^c Optical band gap from the onset of the longest wavelength absorption maximum. Absorption spectra were recorded on dedoped films on ITO glass.

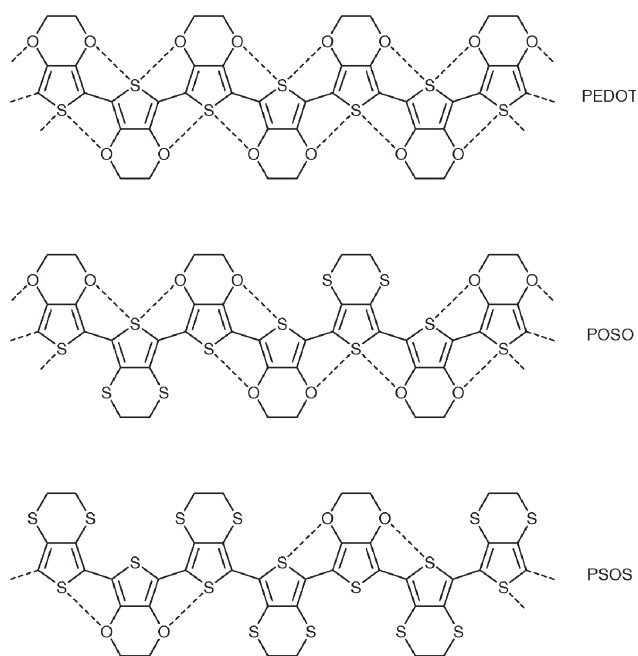


Fig. 7 Expected O...S interactions in segments of all-*anti* conformers.

conjugation still contribute to the redox values of the materials and hence cause the deviation from linear behaviour. The most readily oxidised polymer is PEDOT and the highest oxidation value is seen for PEDTT; this is due to the resonance contribution of the chalcogen atoms and the stronger stabilisation effect of oxygen in comparison to sulfur. A similar chalcogen effect is observed in the oxidation values for the redox active compounds bis(ethylenedioxy)tetrathiafulvalene and bis(ethylenedithio)tetrathiafulvalene.^{37,38} In the case of the copolymers, the value of E_{1ox} for **POSO** is slightly higher than that of PEDOT (50 mV), but E_{1ox} for **PSOS** is 460 mV less than the value for PEDTT. The reduction potentials of the polymers are less sensitive towards the percentage content of oxygen atoms in the main chain, but there is a large difference between peak maxima of the EDOT containing polymers and the all-sulfur analogue. This feature can be explained by the stronger electron withdrawing inductive effect of the oxygen atoms which lowers the reduction potential.

As previously mentioned, the electrochemical band gaps of the polymers can be deduced from the difference between the onsets of the reduction and oxidation waves. Although the onsets of these peaks are removed from peak maxima by several hundred mV, the values for PEDOT and PEDTT are coincident with those reported in the literature. The band gap for **POSO** is only 0.12 eV higher than that of PEDOT, but the HOMO–LUMO difference for **PSOS** tends much towards PEDTT. The same trend is observed in the optical band gaps deduced from the electronic absorption spectra of the polymers (Table 1).

Spectroelectrochemistry

In each case, successive oxidation of the polymers leads to a decrease in intensity of the π – π^* transition and the

simultaneous generation of a new band at longer wavelengths (Fig. 8). This behaviour is attributed to the generation of polarons and bipolarons in the conjugated chain. The polaronic signature is difficult to pick out for PEDTT but is clearly observed in the spectra of PEDOT (850–860 nm), **POSO** (830–840 nm) and **PSOS** (700–740 nm). As expected from the cyclic voltammograms of the polymers, the absorption spectra do not change significantly until the corresponding E_{1ox} potential is reached. In order of increasing potential, the trend for spectroelectrochemical change is PEDOT < **POSO** < **PSOS** < PEDTT. For the polymers PEDOT and PEDTT, the maxima of the new bands extend into the near-IR, but those for the copolymers reach a maximum at lower wavelengths: 840 nm for both **POSO** and **PSOS**. PEDOT is very well known for its transparency in the doped state (the π – π^* band at 578 nm is almost completely lost), and it is this feature which makes the polymer an ideal candidate as an electrochromic material. In contrast, PEDTT retains absorption characteristics in the visible region; the peak at 441 nm is depleted, but remains unshifted throughout the oxidation process. **PSOS** has a higher level of transparency than PEDTT, but low intensity bands persist at 420 and 439 nm. In the case of **POSO**, the initial band at 553 nm is greatly diminished upon doping and the level of transparency rivals that of PEDOT. The isosbestic points for the two polymers are 697 nm (PEDOT) and 673 nm (**POSO**). A quantitative comparison of the electrochromic qualities of PEDOT and **POSO** has been determined by optical switching experiments.

For a material to be useful as part of an electrochromic device it must be able to change readily from one state of absorption to the next with relative ease. For applications such as electrochromic windows,⁷ a switching time scale of seconds or longer would be acceptable. However for purposes such as displays, switching times would need to be increased to a millisecond timescale to minimise delay. Further to these considerations it would be necessary for such materials to be stable in strong sunlight and capable of providing many thousands of switches.

The switching capability of electrochemically grown **POSO** was compared to the previously studied PEDOT system.³⁹ The polymers (grown on ITO glass) were subjected to a cyclic potential which continuously altered the state of the polymers from neutral to their fully oxidised forms, as determined by the spectroelectrochemical measurements detailed above. The changes in absorbance of the polymers were monitored at the maximum absorption wavelengths for the corresponding materials. The PEDOT system was grown by cycling the oxidising potential between –1.6 and +2.2 V and provided an average film thickness of 1100 nm, determined by profilometry. **POSO** was grown potentiostatically at +0.80 V over 600 seconds which accumulated a charge of 4.3 mC and gave a film 900 nm in thickness. For both polymers, the greatest contrast ratios were obtained at the slowest potential cycle rate, which allows the majority of the bulk material to undergo the redox process (Fig. 9). In the case of PEDOT, an increase in the scan rate from 5.25 s per switch (0–1050 mV or 1050–0 mV) to 2.20 s per switch resulted in a decrease in change of absorbance from 17% to 7%. When the switch rate (0–1150 mV or 1150–0 mV) for **POSO** was increased from 5.00 s to

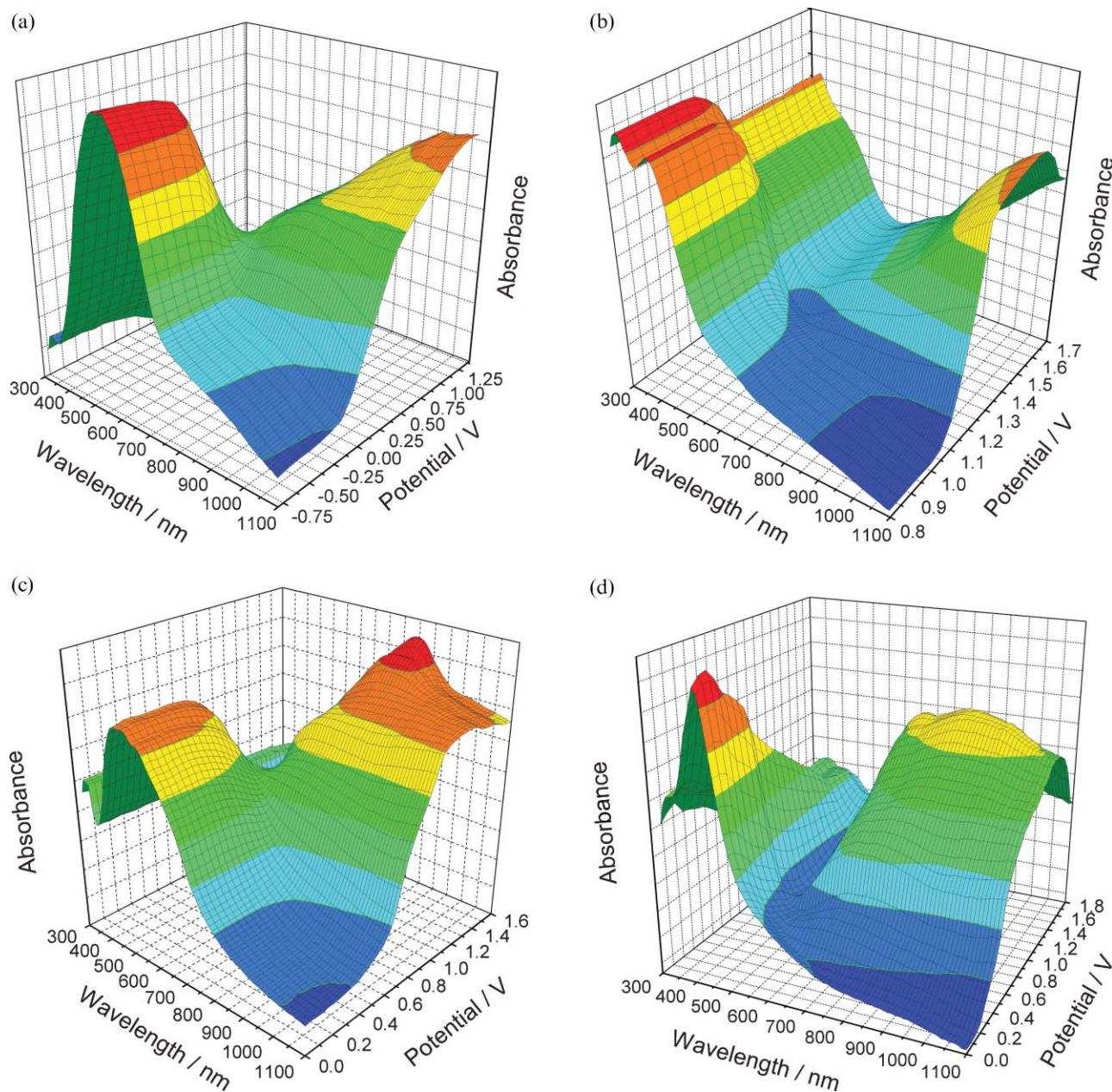


Fig. 8 UV/vis spectroelectrochemical plots for the oxidation of (a) PEDOT, (b) PEDTT, (c) POSO and (d) PSOS.

2.20 s per switch the change in absorbance decreased from 55% to 49% and a further rate increase to 1.25 s per switch saw the change in absorbance drop to 40%. Although the PEDOT system undergoes a much greater drop in absorption at faster scan rates, the results above show that p-doped POSO has greater transparency than PEDOT in the visible region and that the electrochromic effect is more pronounced.

Conclusions

It is clear from this work that the low band gap and low oxidation potential of PEDOT is attributed to a combination of substituent effects and planarity. From our results, we can conclude that the properties of the basic PEDOT structure are tolerant towards the dilution of the EDOT repeat unit in

copolymer assemblies as long as long-range coplanarity is retained. The structure of the polyterthiophene POSO allows for this and there are only relatively small changes in the HOMO–LUMO levels between this polymer and PEDOT. Once long-range planarity is lost, as in the case of PSOS, the differences are much larger. Thus, polyterthiophenes based on structure 5 are of high interest if one desires to impart additional properties to the PEDOT structure, whilst retaining most of the PEDOT character. This conclusion is in agreement with previous studies of polymers incorporating triaryl repeat units with peripheral EDOT units.⁴⁰ The polybithiophene P(EDOT–EDTT) could also provide long-range order, but this would strictly demand a regular, alternating structure, which would be extremely difficult to achieve electrochemically and demanding *via* chemical means.

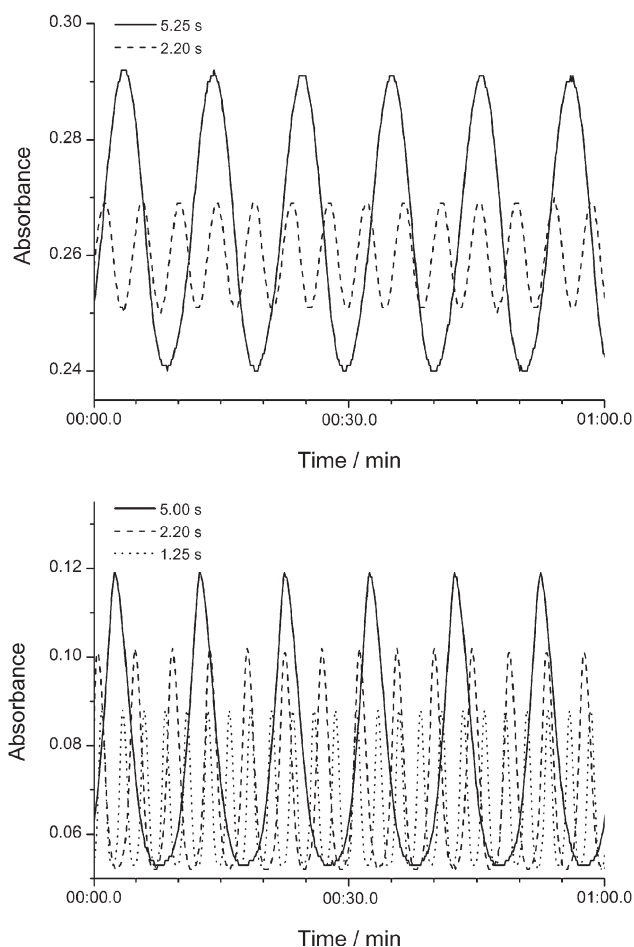


Fig. 9 Change in absorbance upon p-doping at various switching rates for PEDOT (top) and **POSO** (bottom). Absorbance was monitored at the wavelength corresponding to the longest wavelength absorption maximum for each of the polymers.

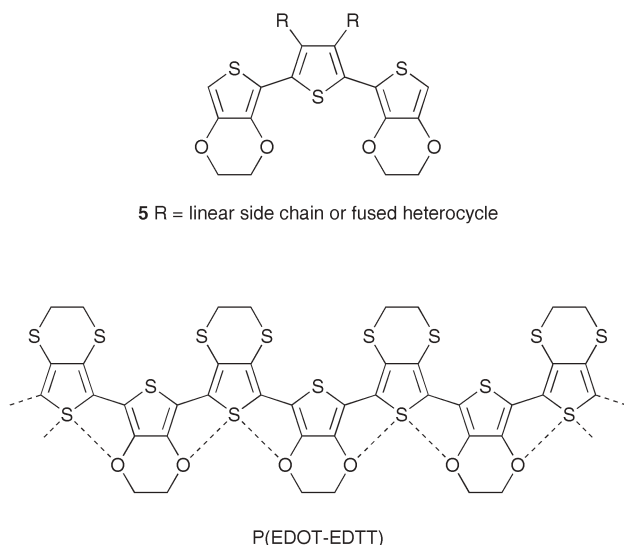


Chart 2

Experimental

General

Melting points were taken using a Stuart Scientific SMP1 Melting Point apparatus and are uncorrected. ^1H and ^{13}C NMR spectra were recorded on a Varian Unity Innova instrument at 300 and 75 MHz; chemical shifts are given in ppm. IR spectra for the characterisation of the compounds were recorded on a ATI Mattson Genesis Series FTIR spectrometer. Mass spectra were recorded on a Micromass Trio 2000 spectrometer. Elemental analyses were obtained on a Carlo Erba Instruments EA1108 elemental analyser. Absorption spectra were measured on a Unicam UV 300 spectrophotometer.

Electrochemistry

Electrochemical measurements were performed on a CH Instruments 660A Electrochemical Workstation with iR compensation, using anhydrous dichloromethane or acetonitrile as the solvent, aqueous Ag/AgCl as the reference electrode and platinum wire and glassy carbon as the counter and working electrodes, respectively. All solutions were degassed (Ar) and contained monomer substrates in concentrations *ca.* 10^{-3} M, together with $n\text{-Bu}_4\text{NPF}_6$ (0.1 M) as the supporting electrolyte. Spectroelectrochemical and switching experiments were conducted on ITO glass.

X-Ray crystallography

Data were collected at 120 K on a Nonius KappaCCD area detector situated at the window of a rotating anode ($\lambda(\text{Mo-K}\alpha) = 0.71073 \text{ \AA}$). The structures were solved by direct methods, SHELXS-97, and refined using SHELXL-97. Hydrogen atoms were included in the refinement, but thermal parameters and geometry were constrained to ride on the atom to which they are bonded. The data were corrected for absorption effects using SORTAV. CCDC reference numbers 280116 and 280117. For crystallographic data in CIF or other electronic format see DOI: 10.1039/b511075k

OSO $\text{C}_{18}\text{H}_{14}\text{O}_4\text{S}_5$, monoclinic, $P2_1$, $a = 9.9758(7)$, $b = 7.6623(3)$, $c = 12.8922(9) \text{ \AA}$, $\beta = 112.418(5)^\circ$, volume = $910.97(10) \text{ \AA}^3$, $Z = 2$, $D_c = 1.657 \text{ Mg m}^{-3}$, $\mu = 0.660 \text{ mm}^{-1}$, $\theta_{\text{max}} = 27.50^\circ$, 7732 measured, 4040 unique ($R_{\text{int}} = 0.0371$) and 3872 ($I > 2\sigma(I)$) reflections, $R1(\text{obs}) = 0.0265$ and $wR2(\text{all data}) = 0.0615$, $\rho_{\text{max}}/\rho_{\text{min}} = 0.284/-0.259 \text{ e \AA}^{-3}$. **SOS** $\text{C}_{18}\text{H}_{14}\text{O}_2\text{S}_4$, orthorhombic, $P2_12_12_1$, $a = 8.1677(13)$, $b = 8.4673(15)$, $c = 27.672(5) \text{ \AA}$, volume = $1913.9(6) \text{ \AA}^3$, $Z = 4$, $D_c = 1.689 \text{ Mg m}^{-3}$, $\mu = 0.837 \text{ mm}^{-1}$, $\theta_{\text{max}} = 27.50^\circ$, 40953 measured, 4382 unique ($R_{\text{int}} = 0.0817$) and 3389 ($I > 2\sigma(I)$) reflections, $R1(\text{obs}) = 0.0710$ and $wR2(\text{all data}) = 0.1501$, $\rho_{\text{max}}/\rho_{\text{min}} = 0.701/-0.383 \text{ e \AA}^{-3}$.

2,5-Bis(3,4-ethylenedioxythiophene)-3,4-ethylenedithiathienophene (OSO)

A THF (15 ml) solution of 3,4-ethylenedioxythiophene (1.30 g, 9.14 mmol) was prepared, placed under a positive pressure of nitrogen and cooled to -78°C . $n\text{-BuLi}$ (2.5 M in hexanes,

3.66 ml, 9.14 mmol) was added dropwise to the solution then left to stir for 0.5 h. A second THF solution (10 ml) of dried zinc chloride was prepared (1.37 g, 10.05 mmol) and was slowly transferred to the first *via* cannula. The zinc chloride containing solution was allowed to stir at -78°C for 1 h further and subsequently warmed to ambient temperature. A third THF solution (15 ml) of 2,5-dibromo-3,4-ethylenedithiathophene **3** (1.52 g, 4.57 mmol) and freshly prepared tetrakis(triphenylphosphine)palladium(0) catalyst (5 mol%, 0.53 g, 0.46 mmol) was also transferred *via* cannula to the main reaction flask and allowed to stir for 0.5 h at room temperature before heating to reflux overnight. (After all cannula transfers are completed, a further 5–10 ml of solvent is flushed through the needle to ensure complete reagent transfer.) The reaction was cooled to room temperature and THF removed. The mixture was redissolved in DCM (75 ml) and washed with saturated ammonium chloride solution (3×100 ml) and water (2×100 ml) before drying and removal of solvent. The product was purified by HPLC eluted with a hexane and ethyl acetate mixture (2 : 1). The crude product was furnished as an orange solid and recrystallised from DCM to give yellow crystals (9%). ^1H NMR (CDCl_3): δ_{H} 6.45 (2H, s), 4.33 (8H, m), 3.24 (4H, s); ^{13}C NMR (CDCl_3): δ_{C} 141.70, 139.04, 126.14, 124.06, 109.85, 99.97, 65.24, 64.75, 28.96; MS (EI): 454 (100%); IR: 3102, 2915, 2874, 1495, 1439, 1365, 1277, 1166, 1067, 1021, 976, 929, 909, 859 cm^{-1} ; Anal. calcd. for $\text{C}_{18}\text{H}_{14}\text{O}_4\text{S}_5$: C, 47.55; H, 3.10; S, 35.27. Found: C, 47.34; H, 3.08; S, 34.06%; Mp 193°C .

2,5-Bis(3,4-ethylenedithiathophene)-3,4-ethylenedioxythiophene (SOS)

The same procedure was utilised as for **OSO**, except 3,4-ethylenedithiathophene and 2,5-dibromo-3,4-ethylenedioxythiophene were used. The target compound **SOS** and bis(EDTT)⁴¹ as a side product were isolated by flash chromatography on a silica column eluted with petrol and DCM (4 : 1) as yellow and green solids respectively and purified by recrystallisation from DCM. Solution 1: EDTT (2.11 g, 12.01 mmol), *n*-BuLi (2.5 M, 5.61 ml, 12.01 mmol) and THF (30 ml). Solution 2: zinc chloride (1.65 g, 12.10 mmol) and THF (10 ml). Solution 3: DBEDOT **4** (1.81 g, 6.05 mmol), $\text{Pd}(\text{PPh}_3)_4$ (5 mol%, 0.210 g, 0.182 mmol) and THF (20 ml).

SOS: Yield (7%); ^1H NMR (CDCl_3): δ_{H} 7.04 (2H, s), 4.42 (4H, s), 3.30 (8H, m); ^{13}C NMR (CDCl_3): δ_{C} 138.45, 126.13, 118.18, 109.93, 65.06, 29.11, 27.97; MS (CI): 487 (11%), 217 (98%), 189 (100%), 84 (51%); IR: 1502, 1450, 1442, 1407, 1361, 1312, 1282, 1084, 855 cm^{-1} ; Anal. calcd. for $\text{C}_{18}\text{H}_{14}\text{O}_2\text{S}_7$: C, 44.41; H, 2.90; S, 46.11. Found: C, 44.01; H, 2.58; S, 45.12%; Mp 245°C .

Bis(EDTT): Yield (8%); ^1H NMR (CDCl_3): δ_{H} 7.11 (2H, s), 3.27 (8H, s); ^{13}C NMR (CDCl_3): δ_{C} 126.60, 126.31, 125.38, 119.60, 28.44, 27.74; MS (CI): 347 (100%), 290 (20%), 246 (17%), 201 (16%), 93 (19%), 69 (20%); IR: 1455, 1405, 1279, 1262, 1041, 935, 853 cm^{-1} ; Anal. calcd. for $\text{C}_{12}\text{H}_{10}\text{S}_6$: C, 41.57; H, 2.91; S, 55.51. Found: C, 41.67; H, 3.27; S, 54.79%; Mp $174\text{--}176^{\circ}\text{C}$ (lit. 178°C).⁴¹

References

- S. Kirchmeyer and K. Reuter, *J. Mater. Chem.*, 2005, **15**, 2077.
- F. Jonas and L. Schrader, *Synth. Met.*, 1991, **41**, 831.
- I. Winter, C. Reese, J. Hormes, G. Heywang and F. Jonas, *Chem. Phys.*, 1995, **194**, 207.
- A. Elschner, H. W. Heuer, F. Jonas, S. Kirchmeyer, R. Wehrmann and K. Wussow, *Adv. Mater.*, 2001, **13**, 1811.
- K. Book, H. Bassler, A. Elschner and S. Kirchmeyer, *Org. Electron.*, 2003, **4**, 227.
- X. Crispin, S. Marciniak, W. Osikowicz, G. Zotti, A. W. D. Van der Gon, F. Louwet, M. Fahlman, L. Groenendaal, F. De Schryver and W. R. Salaneck, *J. Polym. Sci., Part B: Polym. Phys.*, 2003, **41**, 2561.
- H. W. Heuer, R. Wehrmann and S. Kirchmeyer, *Adv. Funct. Mater.*, 2002, **12**, 89.
- H. J. Ahonen, J. Kankare, J. Lukkari and P. Pasanen, *Synth. Met.*, 1997, **84**, 215.
- M. Dietrich, J. Heinze, G. Heywang and F. Jonas, *J. Electroanal. Chem.*, 1994, **369**, 87.
- Y. H. Ha, N. Nikolov, S. K. Pollack, J. Mastrangelo, B. D. Martin and R. Shashidhar, *Adv. Funct. Mater.*, 2004, **14**, 615.
- D. M. Welsh, A. Kumar, E. W. Meijer and J. R. Reynolds, *Adv. Mater.*, 1999, **11**, 1379.
- B. D. Reeves, B. C. Thompson, K. A. Abboud, B. E. Smart and J. R. Reynolds, *Adv. Mater.*, 2002, **14**, 717.
- B. D. Reeves, C. R. G. Grenier, A. A. Argun, A. Cirpan, T. D. McCarley and J. R. Reynolds, *Macromolecules*, 2004, **37**, 7559.
- L. Huchet, S. Akoudad and J. Roncali, *Adv. Mater.*, 1998, **10**, 541.
- H. Brisset, A. E. Navarro, C. Moustrou, I. F. Perepichka and J. Roncali, *Electrochem. Commun.*, 2004, **6**, 249.
- C. L. Gaupp and J. R. Reynolds, *Macromolecules*, 2003, **36**, 6305.
- A. Berlin, G. Zotti, S. Zecchin, G. Schiavon, B. Vercelli and A. Zanelli, *Chem. Mater.*, 2004, **16**, 3667.
- Y. Lee, S. Sadki, B. Tsuie, P. Schottland and J. R. Reynolds, *Synth. Met.*, 2001, **119**, 77.
- G. A. Sotzing, J. R. Reynolds and P. J. Steel, *Chem. Mater.*, 1996, **8**, 882.
- F. Wang, M. S. Wilson, R. D. Rauh, P. Schottland, B. C. Thompson and J. R. Reynolds, *Macromolecules*, 2000, **33**, 2083.
- J. Cao, J. W. Kampf and M. D. Curtis, *Chem. Mater.*, 2003, **15**, 404.
- C. Wang, J. L. Schindler, C. R. Kannevurf and M. G. Kanatzidis, *Chem. Mater.*, 1995, **7**, 58.
- F. Goldoni, B. M. W. Langeveld-Voss and E. W. Meijer, *Synth. Commun.*, 1998, **28**, 2237.
- C. Pozo-Gonzalo, T. Khan, J. J. W. McDouall, P. J. Skabara, D. M. Roberts, M. E. Light, S. J. Coles, M. B. Hursthouse, H. Neugebauer, A. Cravino and N. S. Sariciftci, *J. Mater. Chem.*, 2002, **12**, 500.
- H. J. Spencer, R. Berridge, D. J. Crouch, S. P. Wright, M. Giles, I. McCulloch, S. J. Coles, M. B. Hursthouse and P. J. Skabara, *J. Mater. Chem.*, 2003, **13**, 2075.
- A. Bondi, *J. Phys. Chem.*, 1964, **68**, 441.
- T. Khan, J. J. W. McDouall, E. J. L. McInnes, P. J. Skabara, P. Frère, S. J. Coles and M. B. Hursthouse, *J. Mater. Chem.*, 2003, **13**, 2490.
- D. J. Crouch, P. J. Skabara, J. E. Lohr, J. J. W. McDouall, M. Heeney, I. McCulloch, D. Sparrowe, M. Shkunov, S. J. Coles, P. N. Horton and M. B. Hursthouse, *Chem. Mater.*, accepted.
- P. J. Skabara, R. Berridge, K. Prescott, L. M. Goldenberg, E. Ortí, R. Viruela, R. Pou-Amérgo, A. S. Batsanov, J. A. K. Howard, S. J. Coles and M. B. Hursthouse, *J. Mater. Chem.*, 2000, **10**, 2448.
- P. T. Henderson and D. M. Collard, *Chem. Mater.*, 1995, **7**, 1879.
- Charge Percolation in Electroactive Polymers, in *Electroactive Polymer Chemistry, Part 1 Fundamentals*, ed. M. E. G. Lyons, Plenum Press, New York, 1994.
- N. Sakmeche, J. J. Aaron, M. Fall, S. Aeiayach, M. Jouni, J. C. Lacroix and P. C. Lacaze, *Chem. Commun.*, 1996, 2723.
- B. Sankaran and J. R. Reynolds, *Macromolecules*, 1997, **30**, 2582.
- H. Huang and P. G. Pickup, *Chem. Mater.*, 1998, **10**, 2212.
- Y. Fu, H. Cheng and R. L. Elsenbaumer, *Chem. Mater.*, 1997, **9**, 1720.

- 36 C. Alemán, E. Armelin, J. I. Iribarren, F. Liesa, M. Laso and J. Casanovas, *Synth. Met.*, 2005, **149**, 151.
- 37 T. Suzuki, H. Yamochi, G. Srdanov, K. Hinkelmann and F. Wudl, *J. Am. Chem. Soc.*, 1989, **111**, 3108.
- 38 D. L. Lichtenberger, R. L. Johnston, K. Hinkelmann, T. Suzuki and F. Wudl, *J. Am. Chem. Soc.*, 1990, **112**, 3302.
- 39 A. Kumar, D. M. Welsh, M. C. Morvant, F. Piroux, K. A. Abboud and J. R. Reynolds, *Chem. Mater.*, 1998, **10**, 896.
- 40 J. Roncali, P. Blanchard and P. Frère, *J. Mater. Chem.*, 2005, **15**, 1589.
- 41 The synthesis of bis(EDTT) has very recently been reported: M. Turbiez, P. Frère, M. Allain, N. Gallego-Planas and J. Roncali, *Macromolecules*, 2005, **38**, 6806.



04070300

Fast Publishing? Ahead of the field

To find out more about RSC Journals, visit

RSCPublishing

www.rsc.org/journals